Biosensors and Bioelectronics 208 (2022) 114227

Contents lists available at ScienceDirect

Biosensors and Bioelectronics

journal homepage: www.elsevier.com/locate/bios

DIRECT^2: A novel platform for a CRISPR–Cas12-based assay comprising universal DNA–IgG probe and a direct lateral flow test

Aleksandr V. Ivanov, Irina V. Safenkova, Anatoly V. Zherdev, Boris B. Dzantiev *

A.N. Bach Institute of Biochemistry, Research Centre of Biotechnology of the Russian Academy of Sciences, Leninsky Prospect 33, 119071, Moscow, Russia

ARTICLE INFO

Keywords:
Biosensor
Cas12
Immunochromatographic test
Trans-Cleavage
DNA-IgG complex
Released reporter

ABSTRACT

CRISPR-Cas12-based biosensors are a promising tool for the detection of nucleic acids. After dsDNA-target-activated Cas12 cleaves the ssDNA probe, a lateral flow test (LFT) is applied for rapid, simple, and out-of-laboratory detection of the cleaved probe. However, most of the existing approaches of LFT detection have disadvantages related to inverted test/control zones in which the assay result depends not only on the cleavage of the probe but also on the second factor: the binding of the non-cleaved probe in the control zone. We proposed a novel platform for the detection of trans-cleaved DNA using a universal DNA-IgG probe and LFT with the sequential direct location of test and control zones. The advantage of the platform consists of the assay result depending only on the cleaved probe. For this, we designed a composite probe that comprise two parts: the DNA part (biotinylated dsDNA connected to ssDNA with fluorescein) (FAM), and the antibody part (mouse anti-FAM IgG). The Cas12, with guide RNA, was activated by the dsDNA-target. The activated Cas12 cleaved the probe, releasing the ssDNA-FAM-IgG reporter that was detected by the LFT. The sandwich LFT was proposed with anti-mouse IgG adsorbed in the test zone and on the surface of gold nanoparticles. We called the platform with direct location zones and direct analyte-signal dependence the DNA-Immunoglobulin Reporter Endonuclease Cleavage Test (DIRECT^2). Therefore, this proof-of-concept study demonstrated that the combination of the proposed DNA-IgG probe and direct LFT opens new opportunities for CRISPR–Cas12 activity detection and its bioanalytical applications.

1. Introduction

In recent years, CRISPR–Cas-based biosensors for nucleic acid detection have been explosively developed (Zhang et al., 2021b). These assays include several stages: recognition of the dsDNA target by the Cas12:guideRNA (gRNA) and, as a result, activation of the trans-acting nuclease activity of the Cas12, cleavage of the single-stranded (ss) DNA probe, and detection of cleaved probe. Cas12-based sensors can operate with the dsDNA targets without its amplification using electrochemical (Gong et al., 2021; Zeng et al., 2021) or fluorescent (Liang et al., 2021) amplification of analytical signal. However, most Cas12 biosensors require an amplification of target dsDNA to boost sensitivity (Fu et al., 2021; Glokler et al., 2021). The cleaved probe can be detected by different methods. Lateral flow test (LFT) coupled with CRISPR–Cas provided the most convenient tool for point-of-care (POC) application (van Dongen et al., 2020; Wu et al., 2021). Most designed approaches for LFT detection are based on inverted test/control zones in which the assay result depends not only on the cleavage of the probe but also on the second factor: the binding of the non-cleaved probe in the control zone.

Recently, a DETECTR (DNA Endonuclease Targeted CRISPR Trans Reporter) was proposed for the Cas12-based assay. This platform was designed based on the cleavage of a short (5–15 nt) ssDNA reporter modified by either fluorescent tag and a quencher for fluorescent detection or affinely recognizable tags (e.g. fluorescein [FAM] and biotin) for LFT (Chen et al., 2018). The DETECTR is based on an LFT strip with inverted test/control zones locations; an analyte passes through the control zone and then the test zone. The control zone contains an adsorbed streptavidin that affinity binds biotin, and the test zone contains adsorbed antibodies specific to mouse IgG (anti-mouse-IgG) that binds the conjugate of gold nanoparticles (GNPs) with the mouse antibodies specific to FAM (anti-FAM-IgG). Thus, the FAM-biotin probe non-cleaved by the Cas12 would form a colored ternary complex in the control zone: adsorbed streptavidin–FAM-biotin probe–conjugate of anti-FAM-IgG-GNPs. Upon proper concentration of the probe, streptavidin, and GNP-anti-FAM-IgG conjugate, all

* Corresponding author.
E-mail address: dzantiev@inbi.ras.ru (B.B. Dzantiev).

https://doi.org/10.1016/j.bios.2022.114227
Received 30 December 2021; Received in revised form 17 March 2022; Accepted 25 March 2022
Available online 30 March 2022

non-cleaved probes were captured in the control zone. If the Cas12 was activated and the cleaved ssDNA probe, some portions of the GNP-anti-FAM-IgG conjugate would bind the FAM-labeled products of the cleavage and pass through the control zone, and are bound in the test zone by the anti-mouse-IgG. The DETECTR-based assays with LFT detection were developed for many significant DNA- and RNA-containing pathogens (see reviews (Kostyusheva et al., 2021; Talwar et al., 2021)). In particular, the following pathogens are detected by the LFT-DETECTR: human papillomavirus (Tsou et al., 2019), African swine fever (Bai et al., 2019), SARS-CoV2 (Ali et al., 2020; Brandsma et al., 2021; Broughton et al., 2020; Rezaei et al., 2021), influenza viruses A (Park et al., 2021) and B (Ding et al., 2021; Park et al., 2021), *Mycobacterium tuberculosis* (Wang et al., 2021), myeloproliferative neoplasms (Chen et al., 2021), and potato viruses X and Y (Aman et al., 2020). Gene mutations were also targeted for the DETECTR; Zhang et al., (2021a) proposed an LFT strategy that used an unmutated allele in a spinal muscular atrophy gene as the target for the DETECTR.

An alternative competitive format of the LFT combined with the Cas12 was proposed with the direct order of test and control zone locations. Thus, the test zone contains short poly-A oligonucleotides that bind to the oligo FAM-labeled poly-T reporter. When Cas12 was not activated, the FAM-polyT probe was captured in the test zone and formed a colored ternary complex: adsorbed polyA–FAM-polyT probe–conjugate of anti-FAM-IgG-GNPs. Upon cleavage of the probe, the color intensity in the test zone decreased and the zone became noncolored. The biosensors based on this competitive approach were developed for the detection of *P. aeruginosa* (Mukama et al., 2020a), African swine fever virus (Wu et al., 2020), and human papillomavirus (Mukama et al., 2020b).

For the lateral flow assay, it is well known that simple and user-friendly types of LFTs provide a *direct* target–response relationship (Bahadir and Sezginturk, 2016; Parolo et al., 2020). This means that the signal in the test zone should *directly* depend on the concentration of the cleaved probe and the assay result should depend only on interaction of the cleaved probe in the test zone with an adsorbed receptor and GNP conjugate. This strategy is effectively applied to a wide variety of LFTs from simple sandwich tests to enhanced highly sensitive tests (Gao et al., 2017; Panferov et al., 2018; Zhang et al., 2014). The primary disadvantage of LFT-DETECTR is that test zone captures GNP conjugates regardless probe. Thus, the assay result depends not only on the cleavage of the probe but rather on three factors: (1) interactions of the non-cleaved probe in the control zone with the adsorbed receptor and GNP conjugate, (2) interactions of the cleaved probe with the GNP conjugate, and (3) interactions of the GNP conjugate in any state in the test zone. In result, the interactions of cleaved and non-cleaved probes in control zone determine signal in test zone. Non-optimal condition could cause coloration in test zone that would means false positive results. Some researchers developed Cas12 based LFT where coloration of test zones appeared upon negative samples application (Broughton et al., 2020; Talwar et al., 2021; Tsou et al., 2019; Wang et al., 2020b). Because the result depends on many factors, the probability of obtaining an incorrect result increases. The minority of existing approaches to the Cas-assay with LFT detection are based on a competitive LFT, meaning a *nondirect* target–response relationship. Therefore, a significant improvement to the Cas12-based assay with LFT detection would be a realization of the direct dependence of the signal in the test zone on the cleaved probe concentration based on the interactions of the cleaved probe with the adsorbed receptor and GNP conjugate.

Here, we proposed a novel platform for the detection of cleavage activity of Cas12 based on the universal DNA-IgG probe and an LFT with the direct location of test and control zones. We designed a composite probe that comprises two parts: the DNA part–biotinylated dsDNA connected to ssDNA with FAM, and the antibody part–mouse anti-FAM IgG. The use of the IgG module in this platform for the Cas12-based assay assumes its versatility and applicability in different analyses. The activated Cas12 cleaved the probe, realizing the ssDNA-FAM-IgG reporter that was detected by the sandwich LFT with the anti-mouse IgG adsorbed in the test zone and on the surface of GNPs. As a result, a direct dependence of coloration in the test zone on the amount of analyte was obtained. We called this platform with direct location zones and direct analyte-signal dependence the DNA-Immunoglobulin Reporter Endonuclease Cleavage Test (DIRECT^2). The proof-of-concept study was performed, the dsDNA-target belonging to the genome of *Dickeya solani*, a significant bacterial pathogen of plants (Toth et al., 2011).

2. Material and methods

2.1. Material

Monoclonal mouse antibodies specific to fluorescein (anti-FAM) were produced by Bialexa (Moscow, Russia); streptavidin, protein A, and protein G were produced by Imtek (Moscow, Russia). Non-target monoclonal mouse antibodies to form the control zone of the test strip were produced by Dr. V.G. Avdienko (Moscow, Russia). An anti-mouse IgG-peroxidase conjugate (anti-mouse-HRP) was produced by Jackson Immuno Research Labs (West Grove, PA, USA). Polyclonal goat antibodies against mouse IgG antibodies (amAb1), conjugates of GNPs with anti-mouse-IgG (amAb2), conjugates of GNP-protein A, and GNP-protein G were produced by Arista Biologicals (Allentown, PA, USA). Oligonucleotides with modifications (FAM, 5-carboxyrhodamine-X [ROX], biotin, BHQ, and PEG) were synthetized by Syntol (Moscow, Russia). EnGene LbCas12a, DNAseI, RNAse inhibitor, T7 RNA polymerase, NTP, a Monarch DNA gel extraction kit, and an RNA cleanup kit were purchased from NEB (Ipswich, MA, USA). Tersus polymerase, dNTP, and unmodified oligonucleotides were obtained from Evrogen (Moscow, Russia). Bovine serum albumin (BSA) and $HAuCl_4$ were purchased from Sigma-Aldrich (St. Louis, MO, USA). The membranes for lateral flow strips were produced by Advanced Microdevices (Ambala Cantt, India). Plasmid pGEM-ISG that contains ribosomal intergenic spacer (IGS), 342 bp, from *Dickeya solani* (see Supplementary Materials (SM), Table S1) was obtained in previous research (Ivanov et al., 2020a) and used as a cis-activator (dsDNA target) in the study. Analytical-grade pure salts and organic compounds were used.

2.2. Preparation of conjugate of GNPs with anti-mouse-IgG

GNPs were synthesized according to the modified Frens method by reducing $HAuCl_4$ with sodium citrate (Frens, 1973). The GNP solution with 1.0 absorbance units at 520 nM (OD_{520}) was adjusted to a pH of 9.0. Then, anti-mouse-IgG were added to the GNP solution at a final concentration of 10 μg/mL and stirred for 1 h at 20 °C. The surface of the conjugates was blocked by adding 0.25% BSA (m/w) followed by stirring for 30 min. GNP-IgG conjugates were separated from unbound IgG via centrifugation at 14,000 g for 30 min.

2.3. Preparation of LFT strips and their characterization

The LFT strips were assembled according to Ivanov et al. (2020b) using plastic supports with a CNPC-12 nitrocellulose membrane, a PT R5 glass fiber membrane for the conjugate (conjugate pad), a GFB R4 sample pad, and an AP045 absorbent pad. Either anti-mouse-IgG, protein A, or protein G were dispensed on the test zone, and nonspecific monoclonal mouse antibodies were dispensed on the control zone using an IsoFlow Dispenser (Imagene Technology, USA) with a dispersion rate of 0.15 μL per mm of CNPC-12 nitrocellulose membrane; all components used 1 mg/mL in a 50 mM potassium phosphate buffer, a pH of 7.4 with 100 mM of NaCl (PBS), 10% glycerol, and 0.03% NaN_3 (Safenkova et al., 2020). The synthesized conjugate of GNP–amAb1 (OD_{520} = 3.2), GNP–amAb2, GNP–protein A, or GNP–protein G was dispensed at 26.6 μL per 1 cm^2 of PT R5 membrane. The multimembrane composites were dried after dispensing at 20 °C overnight and then cut into 3.5 mm strips using an Index Cutter-1 automatic guillotine (A-Point Technologies,

USA).

Six types of LFT strips differing in combinations of conjugates and reagents in the test zones were produced: 1) GNP–amAb2 and amAb1, 2) GNP–amAb1 and amAb1, 3) GNP–protein A and protein A, 4) GNP–protein G and protein A, 5) GNP–protein G and protein G, and 6) GNP–protein G and protein A.

The LFT strips were characterized using anti-FAM-IgG with different concentrations (1–1000 ng/mL) in PBS with 0.05% Triton X-100 (PBST). The test strip was dipped in 80 μL of the antibody solution. After 5 min, the test strip was scanned by Canon Scaner (Tokyo, Japan). The color intensities of the test zones were measured by TL120 (Nonlinear Dynamics, Newcastle upon Tyne, UK). A signal of fewer than 2 arbitrary units (arb.u.) was considered below eye-visible level and was set as negative. Data were processed by OriginPro 9.0 (OriginLab, Northampton, MA, USA).

2.4. Synthesis of DNA part of the composite probe for trans-cleavage

The DNA part of the composite probe comprising biotinylated 20 bp of dsDNA (part of eGFP gene), connected to 15 nt of ssDNA with FAM (biotin-dsDNA-ssDNA-FAM), was obtained by annealing complementary oligonucleotides–eGFP-R-20-Bio with eGFP-C3PEG-dT15-FAM (see SM, Table S1). Then, 10 μM of each oligonucleotide was incubated at 80 °C for 2 min then gradually cooled until reaching 20 °C.

2.5. Synthesis of target DNA for trans-cleavage

The construct (600 bp), including the full length IGS and flanked regions, was amplified from the pGEM-IGS plasmid by the PCR according to Ivanov et al. (2020a). The reaction mix contained a Tersus buffer (Evrogen), 200 nM of dNTPs, 200 nM of M13 forward and M13 reverse primers (SM, Table S1), 0.5 ng/μL of pGEM-IGS plasmid, and 30 units of Tersus polymerase. The total PCR volume was 300 μL, and the PCR was performed in 40 cycles. Each cycle was 30 s in length with denaturation at 95 °C, followed by 30 s primers annealing at 55 °C and 60 s elongation at 72 °C. The target product was purified by electrophoresis in 1.5% agarose gel then extracted by a Monarch DNA gel extraction kit. The concentration (ng/μL) of the dsDNA fragment was estimated by triplicate measurements using NanoDrop ND-2000 (ThermoFischer Scientific, Waltham, MA, USA). The IGS fragment was verified by sequencing (Syntol).

2.6. Synthesis and verification of gRNA

The design of the gRNAs was performed using CHOPCHOP version 3 online software (Labun et al., 2019). To obtain gRNAs, in vitro transcription was performed according to Lu and Li (2012) with modifications. Briefly, for synthesis of the gRNA (see SM, Table S1), complementary oligonucleotides (gRNA DNA F and gRNA DNA R) containing the T7 promoter followed by 22 bp of the gRNA gene were denatured at 95 °C then annealed by gradually decreasing their temperature. The reaction mix (100 μL) contained 40 mM of Tris-HCl, pH of 8.0, 20 mM of $MgCl_2$, 2 mM of spermidine, 10 mM of DTT, 1.25 mM of each NTP, 0.5 u/μL of RNAse inhibitor, 2.5 u/μL of T7 RNA polymerase, and 2 μM of DNA template. The reaction was performed at 37 °C for 3 h, then 10 μL of DNAseI buffer and 3 U DNAseI were added and incubated for 30 min at 37 °C. The obtained RNAs were purified by an RNA cleanup kit (NEB). DNAse treatment was repeated to remove residuals of the gDNA template that could cause a false positive signal as ssDNA cis-activator (Chen et al., 2018). The integrity of the gRNAs was checked via electrophoresis in 15% of PAAG with 7M urea in a 20 mM Tris-borate buffer with 0.2 mM EDTA (SM, Fig. S1).

2.7. Adsorption of DNA part of probe on microplate

Streptavidin (6 μg/mL in PBS, 50 μL) was adsorbed on the surface of a black, 96-well microplate Fluoro Nunc MaxiSorp (Thermo Fisher Scientific) for 2 h at 37 °C. The microplate was then washed 4 times with 300 μL of PBST per well using an automatic washer, the Thermo-Scientific Wellwash. Then, 50 μL of biotin-dsDNA-ssDNA-FAM in different concentrations (20 nM–1 μM) were diluted in PBST and added to the streptavidin-covered wells, then incubated for 1 h at 37 °C. The concentration of free and bound biotin-dsDNA-ssDNA-FAM was estimated by a measurement of FAM fluorescence. A solution with an unbound probe (50 μL) was mixed with 50 μL of 25 mM Tris-HCl pH 9.0. FAM fluorescence of the surface-bound probe was measured after the addition of 100 μL of the same buffer to the well. FAM fluorescence was measured using an EnSpire Multipurpose plate reader (PerkinElmer, Waltham, MA, USA) (extinction 498 nm, emission 517 nm). The wells were washed by PBST (see above). The surface of the microplate wells was blocked by 1 mg/mL BSA in PBST for 1 h at 37 °C. The excess BSA was removed via PBST washing.

2.8. Formation of DNA–IgG composite probe (three variants)

Three schemes of the complex formation of the DNA part of the composite probe (biotin-dsDNA-ssDNA-FAM, see Section 2.4) and anti-FAM-IgG were tested. The first scheme utilized the incubation of anti-FAM-IgG with biotin-dsDNA-ssDNA-FAM before the complex bound to the streptavidin-covered microplate (Section 2.7). Anti-FAM-IgG was combined with 50 nM of biotin-dsDNA-ssDNA-FAM with molar ratio of 1:1 and 5:1 in PBST and incubated at 37 °C for 30 min. Then, 50 μL of the mix was added to the streptavidin-covered wells as described in Section 2.7.

In the second scheme, 50 μL of anti-FAM-IgG in different concentrations (0–500 ng/mL) in PBST was added to the wells covered by streptavidin–biotin-dsDNA-ssDNA-FAM. The complex was formed at 37 °C for 1 h. Any unbound anti-FAM-IgG was removed by washing, as described previously.

The third scheme implied the addition of anti-FAM-IgG in different concentrations (0–100 ng/mL) in wells after the DNAse or Cas12 cleavage of the biotin-dsDNA-ssDNA-FAM had been performed (see Section 2.11). The anti-FAM-IgG was incubated at 37 °C for 1 h or 1.5 h.

2.9. Fluorescent trans-cleavage assay without microplate

A trans-cleavage assay was performed according to the Cas12 manufacturer manual (NEB, MA, USA)–NEB2.1 buffer with 30 nM of gRNA and 30 nM of EnGene LbCas12a, which were mixed and incubated at 25 °C for 10 min. Then, 500 nM of ROX-dT15-BHQ2 (SM, Table S1) was added as a probe of trans-cleavage. The reaction of the cleavage began upon the addition of the sample with different concentrations (0–5 nM) of IGS dsDNA target at 37 °C. The total volume of the reaction was 30 μL. The kinetic of the ROX fluorescence was detected by Light Cycler 96 (Roche) at a wavelength of excitation of 578 nm and emission of 604 nm. Data were processed by OriginPro 9.0. Hill's sigmoidal function, which was used for fitting the concentration dependence curve. Three standard deviations of null sample signal were used for detection limit estimation.

2.10. Cleavage in microplate using activation-independent endonuclease (DNAseI)

The reaction mix contained 3 U of activation-independent endonuclease (DNAseI) and DNAseI buffer (NEB). The DNAseI digestion was performed in the microplate by the addition of 50 μL of DNAseI in a well with an attached biotin-dsDNA-ssDNA-FAM or DNA-IgG probe (Section 2.8) and incubated at 37 °C for 30–60 min. The fluorescence of FAM for the bound and cleaved probe was performed as described in Section 2.7.

2.11. Trans-cleavage assay in microplate combined with LFT

Before the cleavage, the reactants (Cas12a, gRNA, and dsDNA target) were mixed and incubated as described in Section 2.9. The assay was performed in two schemes: long and short. In the long scheme, Cas12: gRNA was activated by the dsDNA target in a tube for 30 min at 37 °C. Then, 50 μL of the mix was added into the well with the attached composite DNA–IgG probe. Trans-cleavage proceeded for 1 h at 37 °C. During the short protocol, the reaction mix was added to the well covered with the DNA–IgG probe immediately after the addition of the dsDNA target and incubated at 37 °C for 30 min. The reaction mix was transferred to an untreated well containing 30 μL of PBST. The LFT strip was submerged in this well, and a lateral flow assay was performed as described in Section 2.3. The detection limit was found according three-sigma method with the first tested concentration with a signal higher than 3SD of the null control sample. The relative SD (SD% = SD/Value*100%) was calculated for each of measured IGS concentration. The plot of the mean color intensity (y) versus the dsDNA target concentration (x) was approximated with the use of the Origin Pro 9 (OriginLab, USA) by the four-parameter sigmoidal function.

2.12. Chemiluminescent ELISA

After cleavage, the plate's wells after cleavage (Sections 2.10, 2.11) were washed by PBST as described in Section 2.7. Then, 100 μL of anti-mouse-HRP diluted in PBST 1:3000 (v/v) was added and incubated for 1 h at 37 °C. The washing procedure was repeated after the incubation. One hundred μL of SuperSignal ELISA Pico Chemiluminescent Substrate kit (Thermo Fisher Scientific) was added for a chemiluminescence response. The chemiluminescence signals were measured by Zenyth (Biochrom, Cambridge, UK) for 13 min.

3. Results and discussion

3.1. Design of proposed platform

To detect the Cas12 trans-cleaved DNA with the direct location of the LFT zones and the direct dependence of the color signal on the target amount, we proposed the composite probe and LFT design for the cleaved probe detection (Fig. 1). The composite probe contained DNA and antibody parts. The DNA part was a biotin-dsDNA-ssDNA-FAM construct that contained 20 bp of dsDNA with biotin at the 5′ end of one strand and a polyethylene glycol (PEG) linker at the 5′ end of another strand that connected to 15 nt of ssDNA with FAM at the 5′ end (see sequence in SM, Table S1). The antibody part was mouse anti-FAM-IgG that bound to FAM. To implement the assay, the composite probe was bound to a streptavidin-covered surface, namely the microplate wells (Fig. 1).

The dsDNA fragment with a length of 20 bp was designed to distance ssDNA–IgG from the surface and potentially decrease steric hindrance for Cas12 diffusion and cleavage of the probe. After the activation of Cas12 by the dsDNA target, the reaction mix was added to a well with the DNA–IgG probe attached to the surface. The Cas12 cleaved any ssDNA, including the ssDNA fragment of the probe that released the FAM-bound anti-FAM-IgG in a soluble fraction (Fig. 1). The releasing mouse IgG was detected by the LFT owing to the simultaneous capturing of the different IgG epitopes by the polyclonal goat anti-mouse antibodies adsorbed at the test zone and on the GNP surface. As a result, the colored ternary complex (adsorbed anti-mouse-IgG–anti-FAM-IgG–GNP-anti-mouse-IgG conjugate) was formed. The control zone contained non-target monoclonal mouse antibodies to bind the GNP-anti-mouse-IgG conjugate. We proposed the universal probe with a modular composition and the LFT for the cleaved probe detection that could be applied for different CRISPR-Cas12-based assays. We called the proposed platform the DIRECT^2.

We set the following tasks for developing the platform: (1) screening of compounds for LFT, (2) choice of scheme to form the composite DNA–IgG probe on microplate surface, (3) performance of DIRECT^2 and comparison with convenient fluorescent trans-cleavage assay without microplate.

3.2. Optimization of LFT strips

The screening of the compounds binding the mouse anti-FAM-IgG included the comparison of anti-mouse-IgG, protein G, and protein A. Polyclonal anti-mouse-IgG (amAb1, GNP–amAb1, GNP–amAb2) were used to perform two combinations of LFT strips differing in combination of conjugates and reagents in the test zones: 1) GNP–amAb2 and amAb1 and 2) GNP–amAb1 and amAb1. Protein G and protein A are clearly not suitable for combination with anti-mouse-IgG in the sandwich LFT because both would interact with antibodies. For both proteins, closely spaced epitopes on the Fc IgG are known as the main binding sites for antibodies (Kato et al., 1995; Sauer-Eriksson et al., 1995). However, for both proteins, not only is high domain affinity known, but also are additional binding sites in certain VH (protein A) and CH (protein G) domains. Therefore, we performed all four possible combinations for protein G and A: 3) GNP–protein A and protein A, 4) GNP–protein G and protein A, 5) GNP–protein G and protein G, and 6) GNP–protein G and protein A. The comparison of LFT strips was conducted using anti-FAM-IgG with concentrations from 1 to 1000 ng/mL (Fig. 2). Only the polyclonal IgG sandwich design of the LFT (combinations 1 and 2) was able to detect anti-FAM in this concentration range. The combination (1) detected the antigen from 51.6 ng/mL (Fig. 2., Fig. S2). The combination (2) was more sensitive and had a detection limit that was equal to 4.9 ng/mL of anti-FAM-IgG (Fig. 2, Fig. S2). This difference demonstrates that anti-mouse-IgG from other manufacturers may differ in properties. Other combinations either showed no signal (3, 5, 6) or caused aggregation of the GNP and a pronounced false positive signal (4) (Fig. 2). Recognition sites of protein A and protein G partially overlapped on the Fc domain of an IgG molecule according to Kato et al. (1995), Sauer-Eriksson et al. (1995) and interfered with each other; this was significant for LFT detection. In summary, the binding of anti-FAM-IgG by polyclonal anti-mouse antibodies in a sandwich format was appropriate for LFT detection of releasing anti-FAM-IgG.

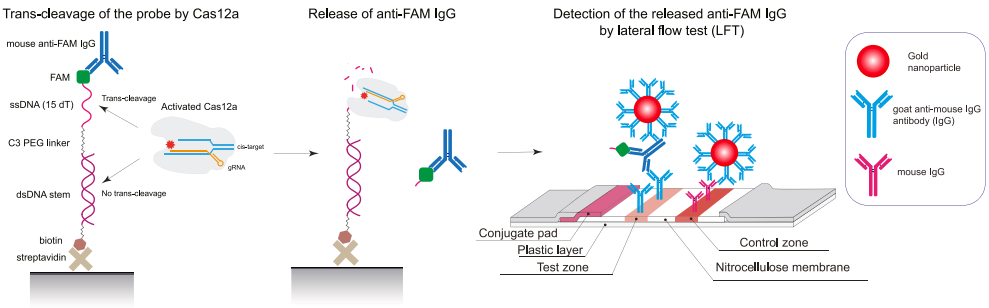

Fig. 1. Scheme of proposed platform – (DIRECT^2) to detect Cas12 trans-cleavage activity.

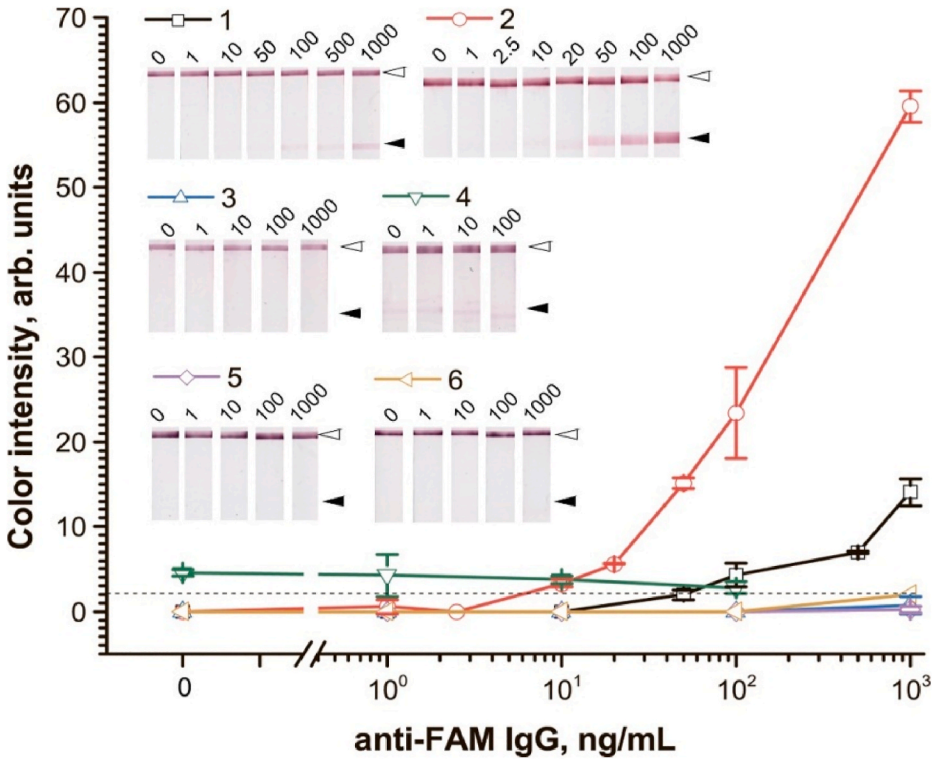

Fig. 2. Lateral flow test strips for anti-FAM IgG detection using different combinations of GNP conjugate and protein adsorbed in test zone: 1) GNP–amAb2 and amAb1, 2) GNP–amAb1 and amAb1, 3) GNP–protein A and protein A, 4) GNP–protein G and protein A, 5) GNP–protein G and protein G, and 6) GNP–protein G and protein A. White triangle notes show the control zone; black triangle notes show the test zone. Dash line represents eye-visible signal (2 arb.u.).

Combination 2 was selected for the following application.

3.3. Choice of scheme to form composite DNA–IgG probe on microplate surface

We chose the concentration of the DNA part of the probe, anti-FAM-IgG, and the sequence of their addition during the probe assembling optimization. The formation of the DNA–IgG probe was optimized for a streptavidin-covered microplate surface. First, the optimal amount of biotin-dsDNA-ssDNA-FAM for binding to the microplate surface was determined. We compared different concentrations of the biotin-dsDNA-ssDNA-FAM upon saturation of the plate wells surface and found that all tested concentration ranges demonstrated saturation from 10 nM. We used an excess of the probe, and most of the biotin-dsDNA-ssDNA-FAM remained unbound in the soluble fraction for each concentration (Fig. S3A). The DNAseI digestion of the surface-bound biotin-dsDNA-ssDNA-FAM demonstrated the same release amount of FAM at a concentration of 50 nM (Fig. S3B). Therefore, 50 nM of biotin-dsDNA-ssDNA-FAM was chosen for the saturation of the streptavidin-covered surface.

Three schemes to form the composite DNA–IgG probe on the microplate surface were proposed and compared. To assess the effectiveness of the formation of the DNA–IgG probe, an endonuclease (DNAseI) treatment was performed that provided a total cleavage of the DNA part of the probe and released the IgG part. The first implied preliminary formation of the biotin-dsDNA-ssDNA-FAM–anti-FAM IgG complex in the solution was followed by a binding of the complex to a streptavidin-coated well and then a washing of unbound molecules (Fig. 3A). Two ratios were tested: 1:1 (50 nM) and 1:5 (50 nM of the probe and 250 nM of anti-FAM-IgG). However, even intensive washing did not remove the background signal in the test zone of the LFT (Fig. 3B). In the case of the 5-fold molar excess of anti-FAM IgG, the background was higher. That strong signal can be explained by the unspecific binding of the excess of anti-FAM IgG with the plate surface. For the first scheme, anti-FAM IgG released after the endonuclease treatment generated an LFT signal over the corresponding background in both tested concentrations of the anti-FAM IgG. However, an excess of anti-FAM IgG increased the background signal, hence lessening the difference between signals in the DNAseI-treated and control samples. Direct fluorescence detection of FAM bound with anti-FAM IgG appeared to be unavailable. The IgG dramatically suppressed FAM fluorescence. To estimate the non-cleaved probes remaining on the microplate, ELISA with chemiluminescent detection was used. The obtained results showed a decrease of anti-FAM IgG on the surface after the DNAseI treatment (Fig. 3C), which proves the LFT results.

The second scheme included a sequential binding of the components, biotin-dsDNA-ssDNA-FAM, then a washing of the unbound biotin-dsDNA-ssDNA-FAM, followed by an addition of anti-FAM IgG (Fig. 3D). Four concentrations of anti-FAM IgG (50, 100, 300, and 500 ng/mL) were tested. After washing the unbound IgG and conducting an endonuclease treatment, LFT strips were used for the detection of the released IgG reporter. No background signal was detected in samples without endonuclease cleavage (Fig. 3E). Positive signals of released IgG reporter correlated with the concentration of used anti-FAM IgG. The amount of detected non-cleaved probes also correlated with the IgG concentration (Fig. 3F).

The third scheme was based on a competition of bound and released FAM for anti-FAM IgG (Fig. 3G). In this approach, the anti-FAM IgG (50, 75, and 100 ng/mL) was added after the endonuclease reaction. The anti-FAM IgG was captured with released FAM or with bound FAM that should be corresponded to a positive or negative LFT signal. However, even when the endonuclease did not cleave the anti-FAM IgG remained in the solution in sufficient quantity to demonstrate the false positive LFT signal (Fig. 3H). Moreover, the extension of incubation time to 1.5 h did not reduce the background signal (Fig. S4A). An analysis of the bound, non-cleaved probe demonstrated the same effect (Fig. 3I, Fig. S4B).

Upon the design of assembling strategies, we suggested two

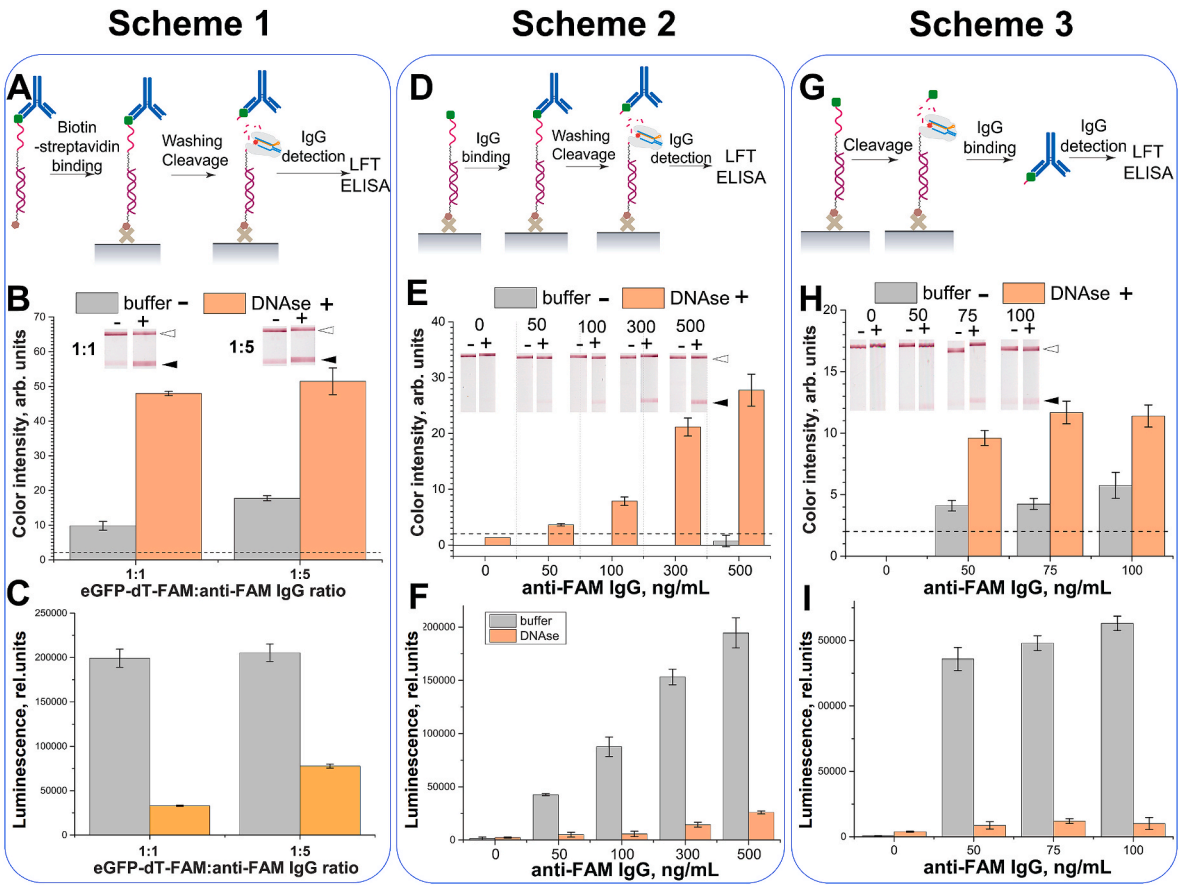

Fig. 3. Schemes of the composite DNA–IgG probe assembling on microplate surface: (1) Preliminary binding of DNA with IgG before surface immobilization; (2) Sequential binding of DNA and IgG with microplate with adsorbed streptavidin before endonuclease treatment; (3) IgG binding after endonuclease treatment of immobilized DNA part of the probe. A, D, G – graphical abstract of the schemes, B, E, H – LFT detection of released IgG reporter, C, F, I – ELISA of surface bound non-cleaved probe. White triangle notes show the control zone; black triangle notes show the test zone. Dash line represents eye-visible signal (2 arb.u.).

challenges: background signal and lower accessibility of ssDNA fragment for an endonuclease. The first issue appeared as a false positive signal and can be caused by an excess of the protein part of the probe, an unspecific binding to the surface followed by dissociation, the dissociation of a reporter protein from its partner, or the dissociation of a dsDNA stem. The problem of excess and unspecific binding can be solved by the optimization of the washing procedure and the selection of a blocking agent. Summarizing the optimization experiments, we chose the second scheme with sequential binding of the biotin-dsDNA-ssDNA-FAM and anti-FAM IgG (500 ng/mL) on the microplate surface before the endonuclease treatment. This scheme demonstrated no false positive signal and a high LFT response after the endonuclease cleavage. Obviously, the scheme can be modified further. Thus, the interaction of the chosen pair (FAM–anti-FAM-IgG) was characterized by K_D equal to 1.5 $\times 10^{-8}$ M (for clone 2A3c according to the manufacturer). It is likely that a more affine pair could enable the increase of anti-FAM IgG upon the composite probe assembly because a less complex dissociation would occur during stage of incubation with the activated Cas12. Moreover, a protein tag covalently bound to DNA could increase the stability of the probe. Extending the length of the ds and ssDNA parts can improve the accessibility of the Cas12 to the cleavage region. Additionally, the use of longer dsDNA can decrease the dissociation of its strands.

3.4. *Performance of DIRECT^2 and comparison with convenient fluorescent trans-cleavage assay without microplate*

To perform the proposed DIRECT^2 for Cas12 trans-cleavage activity detection, we used an IGS dsDNA target. The addition of the dsDNA target activated the Cas12:gRNA complex. Primarily, we estimated the amount of target required to activate the Cas12:gRNA complex in a convenient fluorescent trans-cleavage assay without a microplate and by using an ROX-dT15-BHQ2 probe. The minimal concentration of IGS dsDNA target for Cas12:gRNA activation was equal to 0.05 nM (Fig. 4A, Fig. S5). We performed DIRECT^2 in long and short forms. The long protocol comprised preliminary activation of Cas12a in the solution for 30 min and then the addition of the DNA–IgG probe attached to the surface for cleavage for 1 h. The short protocol included simultaneous activation and cleavage stages in the well and proceeded for 30 min. For this, the Cas12:gRNA complex was added in the well, then the IGS dsDNA target was entered into the reaction. For long protocol, first concentration when all repeated measurement reliably differs from negative samples (more than sum of negative mean value and SD) was 0.05 nM. The long protocol of DIRECT^2 was characterized by LOD equaled to 0.5 nM of the dsDNA target, while the short protocol had LOD equaled to 1 nM of the dsDNA target (Fig. 4B). The obtained concentration dependence for long protocol was approximated with sigmoidal curve (R^2 = 0.98098) (Fig. S6). The precision of measurements was estimated using relative standard deviation (SD%). Most of the measurements in the long protocol of DIRECT^2 had SD% in the range of 16–28% (Table S2). For the short protocol, the range of SD% had wider dispersion but also did not exceed 22.8% (Table S2). At the same time, ELISA with the chemiluminescent detection of a non-cleaved probe on the surface did not provide a reliable signal to separate the negative and positive samples (Fig. S7).

No background signal in the control sample without the dsDNA target was detected in the long form of DIRECT^2. The rapid protocol

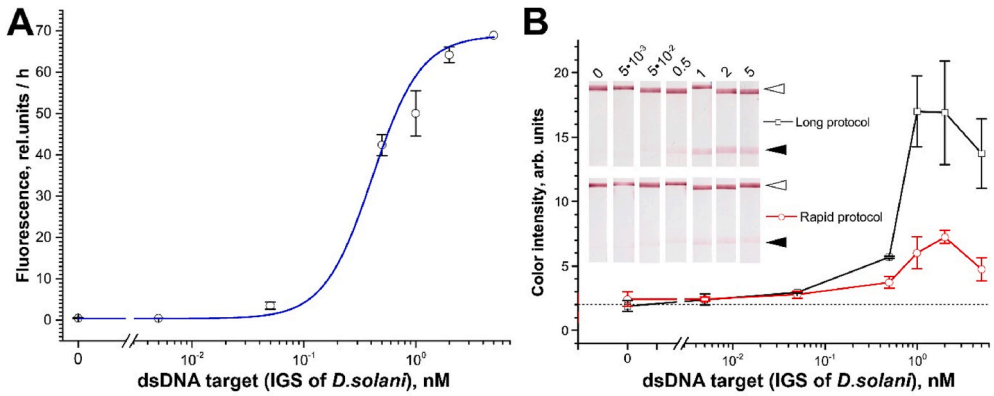

Fig. 4. Detection of model IGS dsDNA target by convenient fluorescent trans-cleavage assay without microplate and with ROX-dT15-BHQ2 probe (A), and DIRECT^2 (B). White triangle notes show the control zone, black triangle notes show the test zone. Dash line represents eye-visible signal (2 arb.u.).

demonstrated less pronounced signals and weak background signal near 2 arb.u. Both protocols had a short linear range of response and were rapidly saturated. However, both protocols provided a direct dependence of the coloration in the test zone on the amount of dsDNA target. A comparison of the Cas12 and DNAseI using the DIRECT^2 platform demonstrated an almost equal efficiency of these endonucleases in the long protocol, and 3-fold gain in intensity of the DNAseI in the rapid protocol (Fig. 4B, Fig. S8). These results demonstrated that the conditions of the long protocol were optimal.

Additionally, we proved the possibility of DIRECT^2 with a probe assembled by the first scheme (with the preliminary incubation of the DNA and IgG parts) (Fig. S9). Despite a false positive signal, a variant of equimolar binding of the DNA part of the probe with anti-FAM IgG only demonstrated a significant difference in DIRECT^2 upon the addition of the cis-activator, illustrating that DIRECT^2 functions with probe assembly in different ways.

The successful results of using the DIRECT^2 for cleaved DNA detection were obtained for magnetic particles as carrier for the probe instead microplate (Fig. S10). The detailed description is presented in Supplementary Materials. Thus, the DIRECT^2 platform has prospects for at least a microplate and magnetic particles as carriers.

The developed DIRECT^2 with long protocol has 10-less LOD and the same sensitivity according visual assessment relative to the convenient fluorescent trans-cleavage assay without a microplate and with an ROX-BHQ2 probe. However, because of its use of LFT strips, DIRECT^2 does not require equipment such as a fluorescence detector. Both approaches have a short linear range of target concentration (Fig. 4A and B) that also characterizes original DETECTR (Chen et al., 2018). In terms of configuration, the DIRECT^2 differs from the LFT-DETECTR only in the use of antibodies and a carrier, which will not lead to a significant increase in the cost of the analysis. As for the time required to attach the probe to the carrier, this can be done in advance. These stages could be performed by lyophilizing and prepacking before the operation with Cas12. The combination of the prepacked microplate with the probe, LFT and Cas12 can be applied for development of POC diagnostic kit. DIRECT^2 can be recommended for combination with some isothermal amplification of DNA targets, like proposed tests based on the DETECTR (van Dongen et al., 2020; Wang et al. 2020). The combination of isothermal amplification with DIRECT^2 can significantly increase the sensitivity of the assay.

Previous Cas12-based assays with LFT detection were based on the signal in the test zone, dependent not only on the cleavage of the probe but also on the binding of the non-cleaved probe in the control zone (Chen et al., 2018). This LFT was realized with a reverse scheme and required a fine optimization of the probe amount and probe-binding compounds in LFT strips. Nonoptimal conditions can cause a false positive signal (Gootenberg et al., 2018). Another approach uses the direct order of zones' locations, but the LFT signal is disappears when the trans-cleavage reaction occurs (Mukama et al. 2020a, 2020b; Wu et al., 2020). This approach is less appropriate for a visual diagnostic because it is challenging to discriminate between samples with weak and moderate trans-cleavage activity.

Thus, the proposed probe for DIRECT^2 has not only shown its effectiveness, but it also offers many options for further improvement and evolution. Therefore, the developed DIRECT^2 platform provided for the first time the detection of Cas12 cleavage activity with the direct location of LFT zones and a direct dependence of color signal on the target amount.

4. Conclusion

We developed the first LFT-based platform for the detection of Cas12 trans-cleavage activity with direct order of test and control zones and direct analyte-signal dependence: DIRECT^2. The proposed composite DNA–IgG probe allows for visual identification of the released IgG reporter in the test zone located before the control zone. The direct order avoids concern over an excess of probe or nonoptimal LFT compounds. Our approach requires the carrier and the separation stage. The composite probe must be connected to any surface appropriate for further separation. The modular nature of the platform allows for the possibility of further modification and improvement.

CRediT authorship contribution statement

Aleksandr V. Ivanov: Investigation, Methodology, Visualization, Writing – original draft, Writing – review & editing. **Irina V. Safenkova:** Conceptualization, Project administration, Methodology, Investigation, Writing – original draft, Writing – review & editing. **Anatoly V. Zherdev:** Supervision, Writing – original draft, Writing – review & editing. **Boris B. Dzantiev:** Supervision, Funding acquisition, Writing – review & editing.

Declaration of competing interest

The authors declare that they have no known competing financial interests or personal relationships that could have appeared to influence the work reported in this paper.

Acknowledgments

The study was financially supported by the Ministry of Science and Higher Education of the Russian Federation.

Appendix A. Supplementary data

Supplementary data to this article can be found online at https://doi.

org/10.1016/j.bios.2022.114227.

References

Ali, Z., Aman, R., Mahas, A., Rao, G.S., Tehseen, M., Marsic, T., Salunke, R., Subudhi, A. K., Hala, S.M., Hamdan, S.M., Pain, A., Alofi, F.S., Alsomali, A., Hashem, A.M., Khogeer, A., Almontashiri, N.A.M., Abedalthagafi, M., Hassan, N., Mahfouz, M.M., 2020. iSCAN: an RT-LAMP-coupled CRISPR-Cas12 module for rapid, sensitive detection of SARS-CoV-2. Virus Res. 288, 198129.

Aman, R., Mahas, A., Marsic, T., Hassan, N., Mahfouz, M.M., 2020. Efficient, rapid, and sensitive detection of plant RNA viruses with one-Pot RT-RPA-CRISPR/Cas12a assay. Front. Microbiol. 11, 610872.

Bahadir, E.B., Sezginturk, M.K., 2016. Lateral flow assays: Principles, designs and labels. Trac. Trends Anal. Chem. 82, 286–306.

Bai, J., Lin, H., Li, H., Zhou, Y., Liu, J., Zhong, G., Wu, L., Jiang, W., Du, H., Yang, J., Xie, Q., Huang, L., 2019. Cas12a-based on-site and rapid nucleic acid detection of african swine fever. Front. Microbiol. 10, 2830.

Brandsma, E., Verhagen, H., van de Laar, T.J.W., Claas, E.C.J., Cornelissen, M., van den Akker, E., 2021. Rapid, sensitive, and specific severe acute respiratory syndrome coronavirus 2 detection: a multicenter comparison between standard quantitative reverse-transcriptase polymerase chain reaction and CRISPR-based DETECTR. J. Infect. Dis. 223 (2), 206–213.

Broughton, J.P., Deng, X., Yu, G., Fasching, C.L., Servellita, V., Singh, J., Miao, X., Streithorst, J.A., Granados, A., Sotomayor-Gonzalez, A., Zorn, K., Gopez, A., Hsu, E., Gu, W., Miller, S., Pan, C.Y., Guevara, H., Wadford, D.A., Chen, J.S., Chiu, C.Y., 2020. CRISPR-Cas12-based detection of SARS-CoV-2. Nat. Biotechnol. 38 (7), 870–874.

Chen, J.S., Ma, E., Harrington, L.B., Da Costa, M., Tian, X., Palefsky, J.M., Doudna, J.A., 2018. CRISPR-Cas12a target binding unleashes indiscriminate single-stranded DNase activity. Science 360 (6387), 436–439.

Chen, M., Zhang, C., Hu, Z., Li, Z., Li, M., Wu, L., Zhou, M., Liang, D., 2021. CRISPR/Cas12a-based ultrasensitive and rapid detection of JAK2 V617F somatic mutation in myeloproliferative neoplasms. Biosensors 11 (8), 247.

Ding, R., Long, J., Yuan, M., Zheng, X., Shen, Y., Jin, Y., Yang, H., Li, H., Chen, S., Duan, G., 2021. CRISPR/Cas12-based ultra-sensitive and specific point-of-care detection of HBV. Int. J. Mol. Sci. 22 (9), 4842.

Frens, G., 1973. Controlled nucleation for the regulation of the particle size in monodisperse gold suspensions. Nat. Phys. Sci. (Lond.) 241, 20–22.

Fu, J., Li, J., Chen, J., Li, Y., Liu, J., Su, X., Shi, S., 2021. Ultra-specific nucleic acid testing by target-activated nucleases. Crit. Rev. Biotechnol. https://doi.org/10.1080/07388551.2021.1983757.

Gao, Z., Ye, H., Tang, D., Tao, J., Habibi, S., Minerick, A., Tang, D., Xia, X., 2017. Platinum-decorated gold nanoparticles with dual functionalities for ultrasensitive colorimetric in vitro diagnostics. Nano Lett. 17 (9), 5572–5579.

Glokler, J., Lim, T.S., Ida, J., Frohme, M., 2021. Isothermal amplifications - a comprehensive review on current methods. Crit. Rev. Biochem. Mol. Biol. 56 (6), 543–586.

Gong, H.X., Wu, Y.L., Zeng, R.J., Zeng, Y.Y., Liu, X.L., Tang, D., 2021. CRISPR/Cas12a-mediated liposome-amplified strategy for the photoelectrochemical detection of nucleic acid. Chem. Commun. 57 (71), 8977–8980.

Gootenberg, J.S., Abudayyeh, O.O., Kellner, M.J., Joung, J., Collins, J.J., Zhang, F., 2018. Multiplexed and portable nucleic acid detection platform with Cas13, Cas12a, and Csm6. Science 360 (6387), 439–444.

Ivanov, A.V., Safenkova, I.V., Drenova, N.V., Zherdev, A.V., Dzantiev, B.B., 2020a. Development of lateral flow assay combined with recombinase polymerase amplification for highly sensitive detection of *Dickeya solani*. Mol. Cell. Probes 53, 101622.

Ivanov, A.V., Safenkova, I.V., Zherdev, A.V., Dzantiev, B.B., 2020b. Nucleic acid lateral flow assay with recombinase polymerase amplification: solutions for highly sensitive detection of RNA virus. Talanta 210, 120616.

Kato, K., Lian, L.Y., Barsukov, I.L., Derrick, J.P., Kim, H.H., Tanaka, R., Yoshino, A., Shiraishi, M., Shimada, I., Arata, Y., Roberts, G.C.K., 1995. Model for the complex between protein-G and an antibody Fc fragment in solution. Structure 3 (1), 79–85.

Kostyusheva, A., Brezgin, S., Babin, Y., Vasilyeva, I., Glebe, D., Kostyushev, D., Chulanov, V., 2021. CRISPR-Cas systems for diagnosing infectious diseases. Methods. https://doi.org/10.1016/j.ymeth.2021.04.007.

Labun, K., Montague, T.G., Krause, M., Torres Cleuren, Y.N., Tjeldnes, H., Valen, E., 2019. CHOPCHOP v3: expanding the CRISPR web toolbox beyond genome editing. Nucleic Acids Res. 47 (W1), W171–W174.

Liang, J.J., Teng, P.J., Xiao, W., He, G.B., Song, Q.F., Zhang, Y., Peng, B., Li, G., Hu, L.S., Cao, D.L., Tang, Y., 2021. Application of the amplification-free SERS-based CRISPR/Cas12a platform in the identification of SARS-CoV-2 from clinical samples. J. Nanobiotechnol. 19 (1), 273.

Lu, C., Li, P., 2012. Preparation of short RNA by in vitro transcription. Methods Mol. Biol. 941, 59–68.

Mukama, O., Wu, J., Li, Z., Liang, Q., Yi, Z., Lu, X., Liu, Y., Liu, Y., Hussain, M., Makafe, G.G., Liu, J., Xu, N., Zeng, L., 2020a. An ultrasensitive and specific point-of-care CRISPR/Cas12 based lateral flow biosensor for the rapid detection of nucleic acids. Biosens. Bioelectron. 159, 112143.

Mukama, O., Yuan, T., He, Z.X., Li, Z.Y., Habimana, J.D., Hussain, M., Li, W., Yi, Z.J., Liang, Q.X., Zeng, L.W., 2020b. A high fidelity CRISPR/Cas12a based lateral flow biosensor for the detection of HPV16 and HPV18. Sensor. Actuator. B Chem. 316, 128119.

Panferov, V.G., Safenkova, I.V., Zherdev, A.V., Dzantiev, B.B., 2018. Post-assay growth of gold nanoparticles as a tool for highly sensitive lateral flow immunoassay. Application to the detection of potato virus X. Microchim. Acta 185 (11), 506.

Park, B.J., Park, M.S., Lee, J.M., Song, Y.J., 2021. Specific detection of influenza A and B viruses by CRISPR-Cas12a-based assay. Biosensors 11 (3), 88.

Parolo, C., Sena-Torralba, A., Bergua, J.F., Calucho, E., Fuentes-Chust, C., Hu, L., Rivas, L., Álvarez-Diduk, R., Nguyen, E.P., Cinti, S., Quesada-González, D., Merkoçi, A., 2020. Tutorial: design and fabrication of nanoparticle-based lateral-flow immunoassays. Nat. Protoc. 15, 3788–3816.

Rezaei, M., Razavi Bazaz, S., Morshedi Rad, D., Shimoni, O., Jin, D., Rawlinson, W., Ebrahimi Warkiani, M., 2021. A portable RT-LAMP/CRISPR machine for rapid COVID-19 screening. Biosensors 11 (10), 369.

Safenkova, I.V., Ivanov, A.V., Slutskaya, E.S., Samokhvalov, A.V., Zherdev, A.V., Dzantiev, B.B., 2020. Key significance of DNA-target size in lateral flow assay coupled with recombinase polymerase amplification. Anal. Chim. Acta 1102, 109–118.

Sauer-Eriksson, A.E., Kleywegt, G.J., Uhlén, M., Jones, T.A., 1995. Crystal structure of the C2 fragment of streptococcal protein G in complex with the Fc domain of human IgG. Structure 3 (3), 265–278.

Talwar, C.S., Park, K.H., Ahn, W.C., Kim, Y.S., Kwon, O.S., Yong, D., Kang, T., Woo, E., 2021. Detection of infectious viruses using CRISPR-Cas12-based assay. Biosensors 11 (9), 301.

Toth, I.K., van der Wolf, J.M., Saddler, G., Lojkowska, E., Helias, V., Pirhonen, M., Tsror, L., Elphinstone, J.G., 2011. Dickeya species: an emerging problem for potato production in Europe. Plant Pathol. 60 (3), 385–399.

Tsou, J.H., Leng, Q., Jiang, F., 2019. A CRISPR test for detection of circulating nuclei acids. Transl. Oncol. 12 (12), 1566–1573.

van Dongen, J.E., Berendsen, J.T.W., Steenbergen, R.D.M., Wolthuis, R.M.F., Eijkel, J.C. T., Segerink, L.I., 2020. Point-of-care CRISPR/Cas nucleic acid detection: recent advances, challenges and opportunities. Biosens. Bioelectron. 166, 112445.

Wang, M., Zhang, R., Li, J., 2020a. CRISPR/cas systems redefine nucleic acid detection: Principles and methods. Biosens. Bioelectron. 165, 112430.

Wang, X.J., Ji, P.P., Fan, H.Y., Dang, L., Wan, W.W., Liu, S.Y., Li, Y.H., Yu, W.X., Li, X.Y., Ma, X.D., Ma, X., Zhao, Q., Huang, X.X., Liao, M., 2020b. CRISPR/Cas12a technology combined with immunochromatographic strips for portable detection of African swine fever virus. Commun. Biol. 3 (1), 62.

Wang, Y., Li, J., Li, S., Zhu, X., Wang, X., Huang, J., Yang, X., Tai, J., 2021. LAMP-CRISPR-Cas12-based diagnostic platform for detection of *Mycobacterium tuberculosis* complex using real-time fluorescence or lateral flow test. Mikrochim. Acta 188 (10), 347.

Wu, H., Chen, X., Zhang, M., Wang, X., Chen, Y., Qian, C., Wu, J., Xu, J., 2021. Versatile detection with CRISPR/Cas system from applications to challenges. Trac. Trends Anal. Chem. 135, 116150.

Wu, J., Mukama, O., Wu, W., Li, Z., Habimana, J.D., Zhang, Y., Zeng, R., Nie, C., Zeng, L., 2020. A CRISPR/Cas12a based universal lateral flow biosensor for the sensitive and specific detection of african swine-fever viruses in whole blood. Biosensors 10 (12), 203.

Zeng, R.J., Wang, W.J., Chen, M.M., Wan, Q., Wang, C.C., Knopp, D., Tang, D.P., 2021. CRISPR-Cas12a-driven MXene-PEDOT:PSS piezoresistive wireless biosensor. Nano Energy 82, 105711.

Zhang, C., Li, Z., Chen, M., Hu, Z., Wu, L., Zhou, M., Liang, D., 2021a. Cas12a and lateral flow strip-based test for rapid and ultrasensitive detection of spinal muscular atrophy. Biosensors 11 (5), 154.

Zhang, K.Y., Wu, J.C., Li, Y.N., Wu, Y.R., Huang, T.F., Tang, D.P., 2014. Hollow nanogold microsphere-signalized lateral flow immunodipstick for the sensitive determination of the neurotoxin brevetoxin B. Microchim. Acta 181 (11–12), 1447–1454.

Zhang, Y., Wu, Y., Wu, Y., Chang, Y., Liu, M., 2021b. CRISPR-Cas systems: from gene scissors to programmable biosensors. Trac. Trends Anal. Chem. 137, 116210.